



Contents lists available at [SciVerse ScienceDirect](http://www.sciencedirect.com)

Quaternary Science Reviews

journal homepage: www.elsevier.com/locate/quascirev



Destructive and non-destructive density determination: method comparison and evaluation from the Laguna Potrok Aike sedimentary record

David Fortin ^{a,b,*}, Pierre Francus ^{a,b}, Andrea Catalina Gebhardt ^c, Annette Hahn ^d, Pierre Kliem ^d, Agathe Lisé-Pronovost ^{b,e}, Rajarshi Roychowdhury ^f, Jacques Labrie ^g, Guillaume St-Onge ^{b,e}, The PASADO Science Team ¹

^a Centre Eau, Terre et Environnement, Institut National de la Recherche Scientifique, Québec, Québec, Canada G1K 9A9

^b GEOTOP Research Center, Canada H3C 3P8

^c Alfred Wegener Institute for Polar and Marine Research, Am Alten Hafen 26, 27576 Bremerhaven, Germany

^d Geomorphology and Polar Research (GEOPOLAR), Institute of Geography, University of Bremen, Celsiusstr. FVG-M, D-28359 Bremen, Germany

^e Canada Research Chair in Marine Geology, Institut des sciences de la mer de Rimouski (ISMER), UQAR, Rimouski, Canada

^f Indian Institute of Science Education and Research, Kolkata, Mohanpur 741252, Nadia, West Bengal, India

^g ISMER (Institut des sciences de la mer de Rimouski), Canada

ARTICLE INFO

Article history:

Received 30 November 2011

Received in revised form

2 August 2012

Accepted 26 August 2012

Available online xxx

Keywords:

CT-Scan

XRF

MSCL Grape density

Sediment density

ICDP-project PASADO

ABSTRACT

Density measurements play a central role in the characterization of sediment profiles. When working with long records (>100 m), such as those routinely obtained within the frame of the International Continental Scientific Drilling Program, several methods can be used, all of them varying in resolution, time-cost efficiency and source of errors within the measurements. This paper compares two relatively new non-destructive densitometric methods, CT-Scanning and the coherent/incoherent ratio from an Itrax XRF core Scanner, to data acquired from a Multi-sensor core logger Gamma Ray Attenuation Porosity Evaluator (MSCL Grape) and discrete measurements of dry bulk density, wet bulk density and water content. Quality assessment of density measurements is performed at low and high resolution along the Laguna Potrok Aike (LPA) composite sequence. Giving its resolution (0.4 mm in our study), its high signal to noise ratio, we conclude that CT-Scan provides a precise, fast and cost-efficient way to determine density variation of long sedimentary record. Although more noisy than the CT-Scan measurements, coherent/incoherent ratio from the XRF core scanner also provides a high-resolution, reliable continuous measure of density variability of the sediment profile. The MSCL Grape density measurements provide actual density data and have the significant advantage to be completely non-destructive since the acquisition is performed on full cores prior to opening. However, the quality MSCL Grape density measurements can potentially be reduced by the presence of voids within the sediment core tubes and the dry and bulk density measurements suffers from sampling challenges and are time-consuming.

© 2012 Elsevier Ltd. All rights reserved.

1. Introduction

Density measurements, along with high-resolution photograph and magnetic susceptibility are often considered as routine analysis of sediment cores (e.g., see St-Onge et al., 2007 for a review on the physical properties of sediment cores). Density measurements

allow the calculation of sediment fluxes to a sedimentary basin, the quantification of sediment compaction and de-watering, and can serve as a powerful tool for inter-core correlation within the same sedimentation basin (e.g. Crémer et al., 2002). When working with different core locations and long sediment profiles (>100 m) such as those usually acquired within the frame of International Continental Scientific Drilling Program (ICDP) projects, research teams have to choose what method of density measurement would provide accurate, fast and reliable results at a resolution that is suitable for the intended scientific objectives.

In this paper we compare two relatively new density measurement techniques, the XRF Coherence/Incoherence ratio and density values from CT-Scan to direct density measurements

* Corresponding author. Centre Eau, Terre et Environnement, Institut National de la Recherche Scientifique, Québec, Canada G1K 9A9. Tel.: +1 418 654 2638; fax: +1 418 654 2600.

E-mail address: david.fortin@ete.inrs.ca (D. Fortin).

¹ PASADO Science Team as listed at http://www.icdp-online.org/front_content.php?idcat=1494.

(bulk density, dry density and water content) and density measurements obtained from the Gamma Ray Attenuation Porosity Evaluator from the Multi-sensor core logger (MSCL Grape). All data were acquired from the composite profile of the Potrok Aike Sediment Archive Drilling Project (PASADO) (Zolitschka et al., 2009). Our objective is to evaluate the quality, sources of error and the comparative advantage of the different methods in terms of accuracy of the signal, and time necessary to perform analyses for a sediment profile of more than 100 m. We also interpret and discuss the density variations along the composite sequence from the ICDP deep drilling site Laguna Potrok Aike, Argentina.

2. Material and methods

Laguna Potrok Aike is located in the Pali Aike Volcanic Field, 100 km east of the Andean volcanic arc (Zolitschka et al., 2009). The lake is 100 m deep with a maximum diameter of 3.5 km. Drilling operation took place from September 2008 to November 2008, with a GLAD800 coring system. We present here results obtained on the composite record of drill site 2 (profile 5022-2CP). Details about the core processing strategy can be found in Ohlendorf et al. (2011).

2.1. Multi sensor core logger (MSCL)

Gamma-ray attenuation was measured at 1 cm intervals on whole cores at the laboratory of the Alfred Wegener Institute (Bremerhaven, Germany) using a Multi Sensor Core Logger (MSCL; Geotek Ltd., UK). A beam collimator of 2.5 mm focused through the center of the core was used for all measurements. For density calibration, a liner equipped with a set of aluminium plates of different thicknesses (ranging from 0 mm to full core size) filled with distilled water was used, as described by Best and Gunn (1999). The Geotek MSCL software (Geotek, 2000) was used for the conversion of raw gamma-ray attenuation counts to gamma-ray attenuation densities (Grape densities). The datasets of cores 5022-2A to 5022-2C were compiled into a composite profile named 2CP following the sampling party protocol (see Ohlendorf et al., 2011), for a total of 9525 data points for the entire record.

2.2. Bulk density, dry density and water content

The samples were obtained from a continuous sampling of the composite profile with a 2 cm spatial resolution. In order to obtain volumetric sub-samples of 2.65 cm³, tubes with an inner diameter of 13 mm were pushed into the 2 cm thick sediment slice (Ohlendorf et al., 2011). These fresh sediment samples of known volume were weighted for calculation of the wet (bulk) density. Efforts were made to reduce the presence of voids and air pockets in the samples. The same volumetric samples were freeze dried at –20 °C in open, but covered, vials for 45 h under a vacuum of 0.11 mbar using a Lyovac GT2 freeze-dryer (Steris GmbH, Huerth, Germany) and then weighed for calculation of the dry density. The water content in percentage was calculated as the difference between wet density and dry density since all samples are assumed to be of equal volume. Here, the original profiles are composed of 4457 data points.

2.3. XRF coherence/incoherence ratio

X-ray fluorescence scanning was performed on split cores from the composite profile (see Ohlendorf et al., 2011) at the University of Bremen using an Itrax core scanner (Cox Analytical Systems, Gothenborg, Sweden) equipped with a 200 µm thick flat capillary waveguide for the incident X-ray beams (Croudace et al., 2006).

Measurements were obtained with a molybdenum (Mo) X-ray tube at 30 kV and with current between 18 and 34 mA, optimized for each section, integrating counts for 10 s over 5 mm-thick intervals. While the main use of this instrument is the determination of the geochemical composition of the sediment, the Itrax uses the forward-scattered Compton (incoherent) and the Rayleigh (coherent) lines in order to normalize the results which corrects for tube ageing and other factors affecting the measurements (Croudace et al., 2006). Moreover, the ratio of the Compton and Rayleigh scattered intensities are affected by the average atomic number of the sample, and hence by mineralogical composition, water and organic carbon content (Croudace et al., 2006). Therefore, some authors used this ratio to detect variations in sediment density (e.g., Thompson et al., 2006) or organic matter (Guyard et al., 2007a,b). The original XRF profiles of the composite sequence investigated here are made of 20 258 data points.

2.4. CT-Scan

CT-Scan imagery corresponds to a 2-D or 3-D linear X-ray attenuation pixel or voxel matrix (Duliu, 1999), where higher density and higher atomic numbers results in higher attenuation of X-rays. Tomograms (2-D images perpendicular to the sample) were obtained at the INRS-Québec using a third generation Siemens Somatom Volume Access sliding gantry medical CT-Scanner. Measurements were performed on the U-channel used as the archive core of the composite profile from site 2 (5022-2CP) in the PASADO project, the same U-channels that were used for paleomagnetic analysis (Lisé-Pronovost et al., in this issue) and high resolution XRF studies (Jouve et al., in press). Tomograms were acquired continuously at every 0.4 mm, along a 0.6 mm-thick slice with an overlap from a tomogram to another of 0.2 mm, totalling 3750 images for each 150 cm U-channel section. The U-channels were scanned with X-ray peak energy of 140 kV with 250-mA current, in captured images of the size of 512 × 512 pixels.

Once acquired, the tomograms were transferred into digital DICOM format using a standard Hounsfield scale (HU scale) (Hounsfield, 1973) from –1024 to 3071 (Duchesne et al., 2009), where –1024 correspond to the density of the air, 0 to the density of water and 2500 to the density of calcite (de Montety et al., 2003). Then, a home-made Matlab routine calculated topograms, i.e., longitudinal 2-D image of the U-channel. All topograms were obtained by averaging a 1 mm cross section of every tomogram centred on the middle of the U-channels. The result of these recalculated topograms are 2-D density maps of slices of the U-channels, with a pixel size of 0.4 mm. HU values from these topograms were then extracted along a single line using the ImageJ software. As the U-channels contain a significant numbers of desiccation cracks, all topograms were analysed visually to identify these cracks, and the corresponding low HU values were then removed manually and replaced by empty values. The original CT-Scan profiles used here are made of 266 623 data points.

3. Stratigraphic corrections and resampling strategies

Our dataset corresponds to four different sampling strategies, with different resolutions and integrates significant post-sampling disturbances in the case of the U-Channels. The MSCL data were acquired on full cores, the coherence-incoherence ratio was obtained on half cores directly after splitting the cores; discrete samples were used for the calculation of the water content, bulk and dry density according to the procedure described in Ohlendorf et al. (2011) and the CAT-Scan images were acquired on U-channels that underwent a certain amount of desiccation. This desiccation introduced a non-cumulative sampling error, since each U-channel

was stratigraphically constrained at the time of the sampling. In order to correct some of the U-channel-specific desiccation and compaction errors, some minor stratigraphic corrections were made by wiggle-matching several clear marker beds measured by the MSCL to the CAT-Scan measurements to the same depth using the Analyseries software (Paillard, 1996). These stratigraphic corrections removed some of the error, but a significant amount of mm-scale, non-cumulative error is most likely still present in the datasets, thus potentially reducing the strength of the correlation between CAT-Scan values and the other density measurements.

In order to allow for the comparison between these values all measurements have been mathematically resampled to the lowest resolution dataset. Hence, MSCL Grape densities, Coherence/Incoherence values as well as the CT-Scan values were averaged across the 2 cm thick intervals corresponding to the bulk density, dry density and water content samples. Six density profiles with an identical number of 5030 (minus missing data in some series) data points were therefore obtained allowing the calculation of linear least-square regression coefficient (R^2) between all resampled datasets.

4. Data comparison

Fig. 1 shows the six density proxies using the resampled series. Most major features affecting the density curves of the composite profile such as compaction in the upper twenty metres, tephra layers, laminated sections, etc can be observed. These features are going along with the lithologic units defined by Kliem et al. (in this issue). The two first units, A and B, where compaction is observable in all density proxies are mostly composed of laminated silts and sands, with a larger occurrence of coarse sediments in Unit B. Unit B is also characterized by the presence decimetric graded beds and by

the occurrence, mostly at the base of the unit, of large amounts of aquatic mosses. The remaining of the sequence consists of three sub-units (C-1, C-2 and C-3) which shows an increasing number of mass movement deposits: normally graded beds, ball and pillow structures and structureless sand and fine gravel layers.

When compared to each other through least square relationship we observe that the water content is significantly better correlated with the CT-Scan's HU numbers ($R^2 = 0.83$) and the coherence/incoherence ratio ($R^2 = 0.73$) than are the same measurements with wet density ($R^2 = 0.63$) (Fig. 4). Grape density has essentially the same correlation coefficient with dry density and water content ($R^2 = 0.67$ and 0.68 respectively) and a significantly lower one with bulk density ($R^2 = 0.59$). This is a counter intuitive relationship because the measurements of Grape density is directly related to bulk density and not to dry density or water content.

5. Discussion

In order to understand these relationships, we looked at 2 series of 200 contiguous samples representing 4 m of sediment at two selected depth intervals of the composite profile (Fig. 2). Two main sources of error are observable on Fig. 2. First, some minor stratigraphic offsets of the CT-Scan measurements exists relative to the other measurements. For example (Fig. 2, Box A), the arrows points to a small scale decrease in density visible on all different curves but which appears a few centimetres before on the HU series than on the other ones. Other similar offset are noticeable. These discrepancies are due to the post sampling desiccation of the U-channels from which the CT-Scan measurements were obtained as discussed in the previous section. The second type of error is illustrated by the large amount of noise in both dry and bulk density series, compared to the noise that is comparatively absent from the

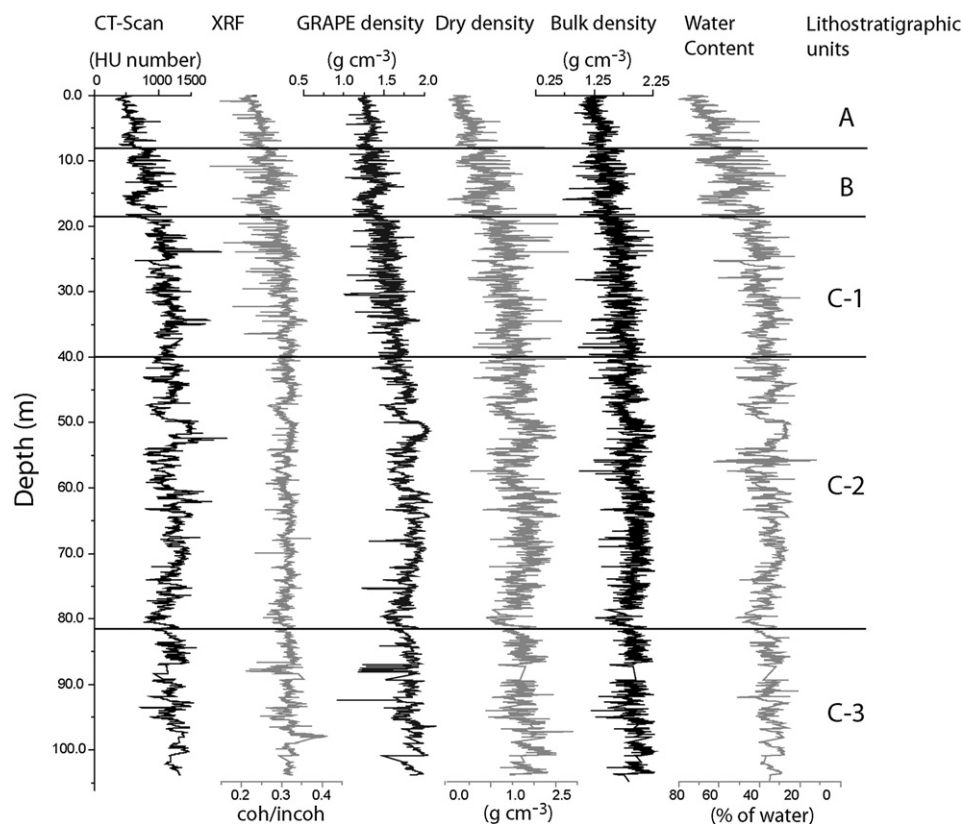


Fig. 1. Time series resampled according to their sample ID. The lithostratigraphic units are described in Kliem et al. (in this issue).

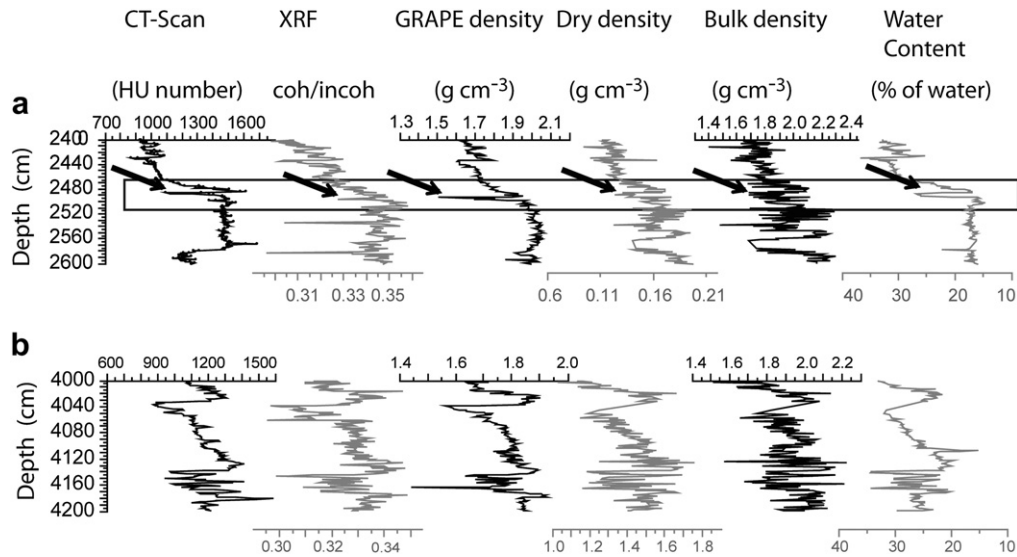


Fig. 2. Two 2 m long intervals (A, B) of the density profile; data are resampled according to the sample ID. The black arrows indicate the same stratigraphic marker in all profiles.

water content series. The source for that noise appears to result from the use of a constant-volume sub-sampling device: the sampling device (in this case 2.65 cm³) is not always completely filled because of the presence of air pockets, cracks and other discontinuities within these samples. These induce a significant error as these measurements are obtained for the weight/volume ratio. This source of error is absent from the water content measurements since they are calculated from the difference of the bulk mass over dry mass of the sub-sample and hence is not mathematically dependent of the volume and its handling errors. Air or water pockets within the full tubes may have induced a similar type of error with the Grape measurements since raw counts are normalized by the core diameter. Finally another source of error can be attributed the drying of the sediments after opening

and during sub-sampling affecting all measures but the Grape density that are performed on full cores.

Because of these significant source of error within the wet and dry density data, the comparative interpretation of the indirect measurements with these two measurements were performed with caution. Although imperfect for representing bulk or dry density, the water content appears to be a more suitable measure for testing the quality of our indirect proxies.

In order to evaluate the datasets at their full potential, two distinct sedimentary facies discussed by *Kliem et al. (in this issue)* were compared using the original resolution of our datasets instead of the 2-cm resolution of the resampled datasets discussed previously (*Fig. 3A, B*). *Fig. 3A* consists of a 41 cm long Holocene laminated pelagic silty sediment interval with sub-centimetre

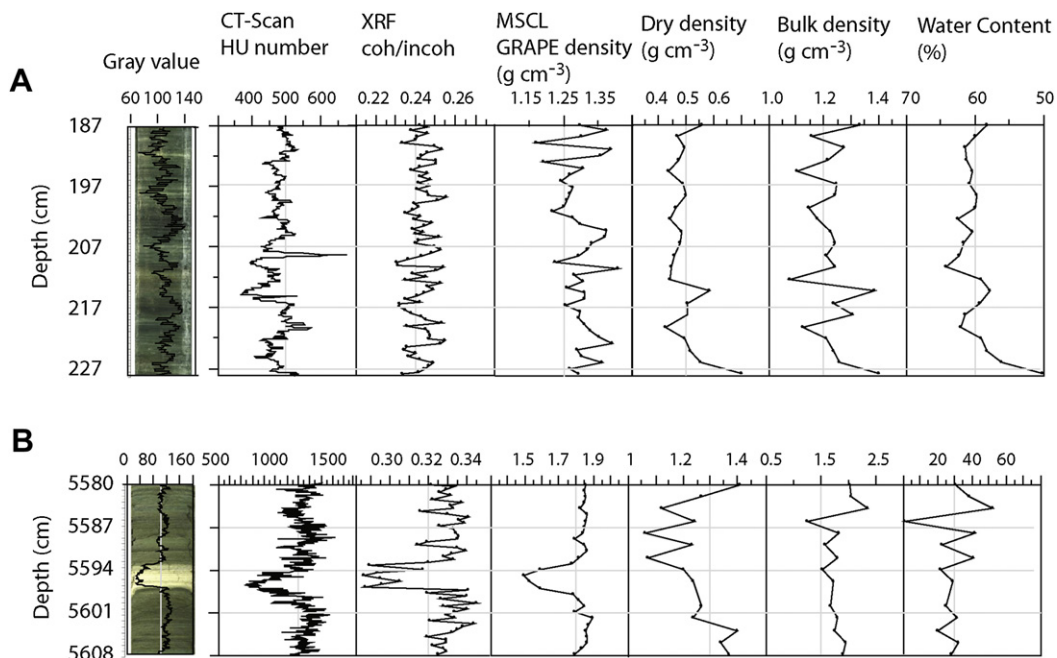


Fig. 3. Density profiles at the original resolution. Two contrasted sedimentary facies: a. Pelagic silty sediments of lithostratigraphic from unit A. b. Thin tephra layer within a fine grained matrix of lithostratigraphic from unit C-2.

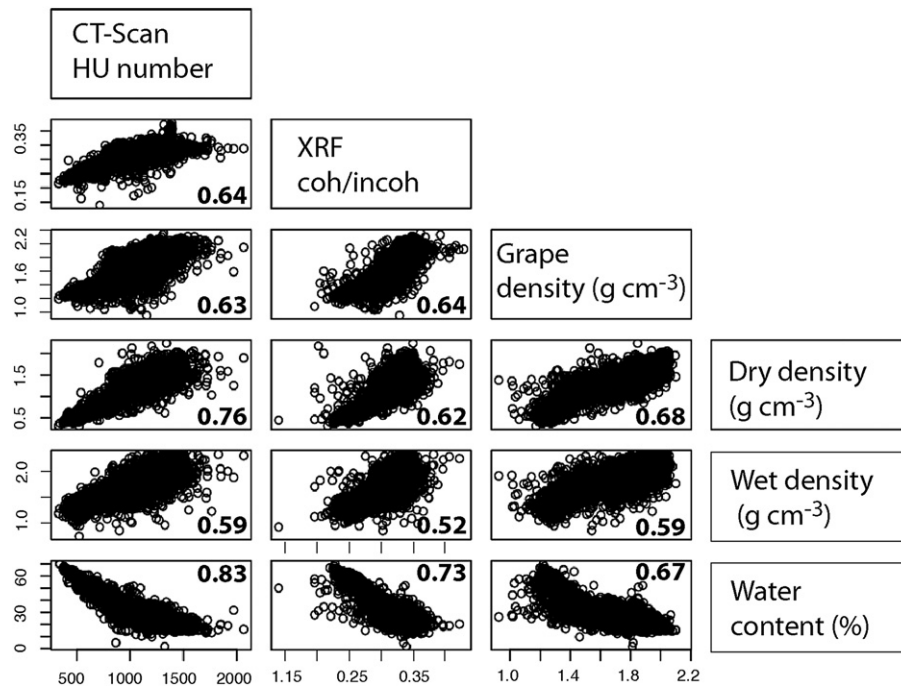


Fig. 4. Scatter plots of the relationship between the independent datasets after resampling according to their sample ID. All resampled data points represent a value integrated over 2 cm, so each dataset have 4750 data points. The numerical values inside the scatter plot boxes are R^2 coefficients (linear least-squared regression).

laminations (lithostratigraphic unit A). This section has a relatively low average density (bulk density 1.2 g/cm^3 , dry density 0.5 g/cm^3). The second interval, see Fig. 3B, shows of a silty tephra layer within a fine grained matrix, with higher densities than in interval A (bulk density 1.8 g/cm^3 , dry density 1.2 g/cm^3). Both intervals are discussed in Fig. 3A and H respectively of Kliem et al. (in this issue). Of the 6 density proxies and measurements, HU presents the best native resolution (0.4 mm) and hence, better captures small scale density variability within the sample. The coherence/incoherence signal and the Grape density datasets with their respective resolution of 5 mm and 1 cm have a too coarse resolution to measure the centimetre-scale density variability such as the fine lamination in the interval of Fig. 5A, but captures well the 3.5 cm thick tephra layer in Fig. 3B. However, due to their 2 cm resolution, none of the direct density and water content measurements performed on the sediments could neither capture small scale density variations nor the tephra layer.

5.1. Evaluation of CT-Scan and Itrax indirect density measurements

In order to evaluate the relationship of each resampled datasets with each other we produced scatter plots and least-square coefficient of these relationships (Fig. 4). As expected, the CT-Scan HU numbers are in good agreement with the water content ($R^2 = 0.83$). However, we can observe from the scatter plot (Fig. 4) that the correlation between HU units and the water content is weakening with increasing densities. We attribute this lower correlation at higher densities to the errors in the discrete sampling described previously. Indeed, assuming a random distribution of error within all samples, the error within high density samples will translate into a larger spread of data points compared to low density samples because this error corresponds to a percentage of the mass per cubic centimetre and hence increase with denser samples.

A good relationship between HU numbers and Grape density ($R^2 = 0.63$) is also observed, the spread around the regression line is quite large although constant confirming that the weakening of the

relationship observed with discrete samples is due to the sampling strategy.

The CT number to wet density relationship has been evaluated previously for a variety of sediments (Orsi et al., 1994; Orsi and Anderson, 1999; Tanaka et al., 2011). This resulted in an essentially perfect correlation between CT numbers and sediment bulk density when using homogenized samples and with virtually no effect of grain size on X-ray attenuation (Orsi and Anderson, 1999) and good overall agreement when using heterogeneous sediment samples (St-Onge and Long, 2009; Tanaka et al., 2011). Calibration experiments have also shown that the presence of CaCO_3 in the

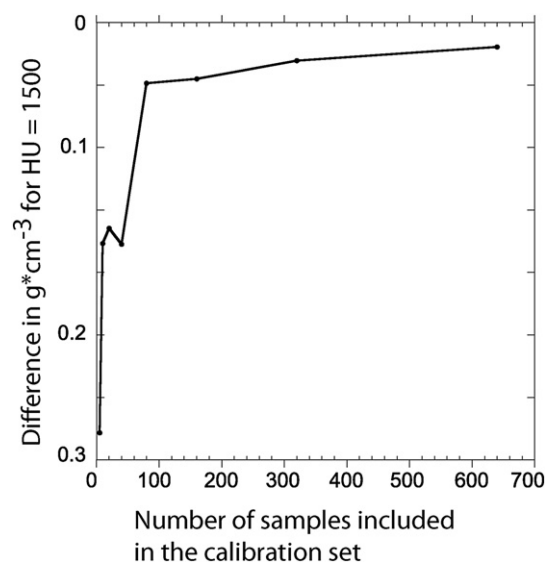


Fig. 5. Sensitivity of the calibration as a function of the number of data points: HU and dry density. The curve represent the difference in estimated dry mass for an HU value of 1500 for a given number of calibration points relative to a calibration performed on the entire dataset of 5030 samples.

sediments can create an offset from SiO₂ rich samples, with higher CT numbers obtained for a given bulk density in calcite rich samples due to an increased attenuation via photoelectric phenomena caused by the higher effective atomic number of carbonate samples (Boespflug et al., 1994; Orsi and Anderson, 1999). Minor stratigraphic offsets, as well as density changes due to post-sampling desiccation of the U-channels might also play an effect in the spread of the relationship between the Grape densities values and the HU values. Hence, CT-numbers obtained from fresh cores immediately before the discrete sampling for H₂O and dry bulk sediment would have likely yielded stronger correlations.

Although noisier than the HU numbers, the coherence/incoherence ratio also provides a good approximation of the water content within the sediments with an overall correlation of 0.73 (R^2). However this relationship does not indicate that the coherence/incoherence ratio can be used as a straightforward for water content since this relationship remains valid only if the sediment composition is constant and the water content changing, which is not the case here. We observe that the correlation between water content and coherence/incoherence ratio is stronger for high water content compared to low water content, due to change in sediment composition and for larger sampling errors with water measurements in low water content intervals as discussed earlier. However, this relationship is weaker compared to HU maybe because the sample measured by the XRF core scanner is even smaller than the one used to compute the HU values, hence exacerbating further the natural heterogeneity of the sediment (e.g. ball and pillow structures, isolated coarse grains). Moreover, the relationship is characterized by more frequent outliers maybe because the incoherence/Coherency ratio is very sensitive to topographic irregularities at the surface of the measured half core sections (Cuven et al., 2007).

Grape density measurements are also well correlated with water content and bulk density ($R^2 = 0.67$ and 0.68 , respectively). Part of the error can be attributed to the desiccation of the cores and cores samples after their opening and during the discrete sampling.

6. Calibration and sensitivity test

Given the diverse sources of error discussed above, any attempt of direct calibration should be taken with caution. However, assuming that the best calibration possible is given by the least-square regression of the entire dataset (5030 data points), we can explore how fewer calibration data points would impact the slope of the regression curve and hence the estimated values. The number of data points necessary to such a calibration is specific to every different sediment cores; very complex sedimentary sequence made of a wide variety of materiel with contrasting densities, such as found in core 5022-2CP, would necessarily require more calibration data points than homogenous sedimentary sequences with little lithologic variability. Hence, a sampling strategy based on the range of densities rather than on a sampling performed at regular interval appears more efficient and possibly more accurate for a similar number of data points. To illustrate this strategy, we used the sub-sampled CT-Scan dataset that we sorted according to the HU numbers (ranging from 2065 to 328). From this ascending HU series, we took a set numbers of samples at regular intervals and regressed them against dry density values. Eight datasets were taken (5, 10, 20, 40, 80, 160, 320 and 640 samples) and each was regressed against the measured dry density values. Fig. 5 shows the difference in g per cubic centimetre between each regression (for a given HU value of 1500) and the regression performed on the entire dataset. We can observe that as few as 64 samples are sufficient to produce a calibration that depart from the

calibration based on the 5030 samples by less than 0.05 g per cubic centimetre and that this difference becomes less than 0.02 g per cubic centimetre when using 640 samples selected along the range of HU values.

6.1. General discussion

This study was the opportunity to assess the reliability of different density measurements on very large datasets. Overall, the six density profiles measured along the composite sequence of Laguna Potrok Aike reveal similar trends and stratigraphic details. However, high-resolution methods such as the CT-Scan present clear advantages for the identification and description of small scale sedimentary facies and structures within the sedimentary record such as centimetre-scale laminations, tephra layers, small graded beds, etc. Our results show that the two indirect density measurements provide a good approximation of the density for the composite profile. HU numbers from the CT-Scan appear to provide the best proxy for dry density and H₂O content, followed by the incoherence/coherence ratio from the XRF core scanner. The relatively weaker relationship between these measurements and discrete density measurements can be attributed to errors in volumetric sampling in this study. Precise bulk density measurements of the sediment, using for example the pycnometer analysis (Tamari, 2004), would have likely yielded a better fit between the measurements, as reported in the literature (Best and Gunn, 1999). CT-scanning, when performed on full cores rather than U-Channel as it is the case in this study, could also provide three-dimensional reconstructions of density variability within a core, a potentially powerful tool to recognise small scale disturbances, and inter-core correlation prior to core opening.

Our results also confirms that the incoherence/coherence ratio from the XRF core scanner can be used with confidence as a proxy of density for long sediment cores presenting a large array of sediment types. XRF core scanning is becoming more widely used for the geochemical characterization of the sediment cores, making this density proxy readily accessible in a number of studies. The use of MCSL Grape density measurements offers the indisputable advantage of being fast, relatively inexpensive and completely non-destructive since it is performed on full cores. However, the quality of the measurements depend on the absence of voids, gas or air pockets within the sediment core tubes.

Both the Itrax core scanner and the CT-Scan are non-destructive and fast technologies allowing measurements of density. Economically, they favourably replace density measurements taken on discrete sample (here 6000) that require intensive labour and that are prone to sampling errors. Moreover, they both provide indirect density measurements at much higher resolution (100 μ m versus 2 cm in this case). For long sedimentary sequences, these new techniques are good alternatives to discrete measurement provided they can be calibrated against carefully sampled volumetric samples.

7. Conclusions

Density measurements of long sediment sequences (>100 m) can represent significant monetary and time investment. Our methodological comparison is demonstrating that measurements on discrete samples must be interpreted with caution since the use of constant volumetric samples (use of a tube of constant diameter pushed into sediment slices) can induce significant measurement errors. We also demonstrate that the XRF coherent/incoherent ratio, although noisier than values obtained from CT-Scanning, can provide an accurate approximation of change in density and of water content of a sediment core. CT-Scans performed on full,

unopened cores, calibrated with discrete measurement of density and water content with the pycnometer appears to be the most recommendable method for density measurement of long sedimentary profiles. The discrete sampling effort can be significantly reduced if the calibration dataset is carefully built to represent replicas of the different lithological units rather than continuous sampling.

Acknowledgements

This research is supported by the International Continental Scientific Drilling Program (ICDP) in the framework of the “Potrok Aike Maar Lake Sediment Archive Drilling Project” (PASADO). Funding for drilling was provided by the ICDP, the German Science Foundation (DFG), the Swiss National Funds (SNF), the Natural Sciences and Engineering Research Council of Canada (NSERC), the Swedish Vetenskapsradet (VR) and the University of Bremen. For their invaluable help in field logistics and drilling we thank the staff of INTA Santa Cruz and Rio Dulce Catering as well as the Moreteau family and the DOSECC crew. David Fortin was financially supported by a postdoctoral fellowship from FQRNT. This project was also made possible by and Discovery grants to P. Francus and G. St-Onge. Many thanks to Dr. Sandrine Solignac fruitful discussions.

References

- Best, A.I., Gunn, D.E., 1999. Calibration of marine sediment core loggers for quantitative acoustic impedance studies. *Marine Geology* 160.
- Boespflug, X., Ross, N., Long, B., Dumais, J.F., 1994. Axial tomodesitometry: correlation between tomographic intensity and density of materials. *Canadian Journal of Earth Sciences* 31 (2), 426–434.
- Crémer, J.-F., Long, B., Desrosiers, G., De Montety, L., Locat, J., 2002. Use of scanography for the study of the density of the sediments and for the characterization of sedimentary structures: the example of deposited sediments in the saguenay river (Quebec, Canada) after the flood of July 1996. *Canadian Geotechnical Journal* 39 (2), 440–445.
- Croudace, I.W., Rindby, A., Rothwell, R.G., 2006. ITRAX: Description and Evaluation of a New Multi-function X-ray Core Scanner. In: Geological Society, London, Special Publications, vol. 267 (1), pp. 51–63.
- Cuven, S., Francus, P., Crémer, J.F., 2007. Protocoles d'utilisation et essais de calibration du scanner de microfluorescence X de type « ITRAXTM Core Scanner », ISBN 978-2-89146-552-6. INRS Eau, Terre et Environnement, rapport de recherche 954.
- de Montety, L., Long, B., Desrosiers, G., Crémer, J.F., Locat, J., Stora, G., 2003. Scanner use for sediment study: the influence of physical parameters, chemistry and biology on tomographic intensities. *Canadian Journal of Earth Sciences* 40 (7), 937–948.
- Duchesne, M.J., Moore, F., Long, B.F., Labrie, J., 2009. A rapid method for converting medical computed tomography scanner topogram attenuation scale to hounsfield unit scale and to obtain relative density values. *Engineering Geology* 103 (3–4), 100–105. <http://dx.doi.org/10.1016/j.enggeo.2008.06.009>.
- Duliu, O., 1999. Computer axial tomography in geosciences: an overview. *Earth-Science Reviews* 48 (4), 265–281.
- Geotek, 2000. Multi-Sensor Core Logger. Geotek, 127 pp. <http://www.geotek.co.uk/>.
- Guyard, H., Chapron, E., St-Onge, G., Anselmetti, F., Arnaud, F., Magand, O., Francus, P., Mélières, M.-A., 2007a. High-altitude varve records of abrupt environmental changes and mining activity over the last 4000 years in the Western French Alps (Lake Bramant, Grandes Rousses Massif). *Quaternary Science Reviews* 26, 2644–2660.
- Guyard, H., Chapron, E., St-Onge, G., Anselmetti, F.S., Arnaud, F., Magand, O., Francus, P., Mélières, M.-A., 2007b. High-altitude varve records of abrupt environmental changes and mining activity over the last 4000 years in the western French alps (lake bramant, grandes rousses massif). *Quaternary Science Reviews* 26 (19–21), 2644–2660.
- Hounsfield, G.N., 1973. Computerized transverse axial scanning (tomography): I. description of system. *British Journal of Radiology* 46 (552), 1016–1022.
- Jouve, G., Francus, P., Lamoureux, S., Provencher-Nolet, L., Hahn, A., Haberzettl, T., Fortin, D., Nuttin, L. The PASADO Science Team. Microsedimentological characterization using image analysis and m-XRF as indicators of sedimentary processes and climate changes during Lateglacial at Laguna Potrok Aike, Santa Cruz, Argentina. *Quaternary Science Reviews*, in press.
- Kliem, P., Enters, D., Hahn, A., Ohlendorf, C., Lisé-Pronovost, A., St-Onge, G., Wastegård, S., Zolitschka, B., The PASADO Science Team. Lithology, Radiocarbon Dating and Sedimentological Interpretation of the 51 ka BP Lacustrine Record from Laguna Potrok Aike, Southern Patagonia, in this issue.
- Lisé-Pronovost, A., St-Onge, G., Gogorza, C., Zolitschka, B., The PASADO Science Team. High-resolution Paleomagnetic Secular Variation and Relative Paleointensity since the Late Pleistocene in Southern South America, in this issue.
- Ohlendorf, C., Gebhardt, A.C., Hahn, A., Kliem, P., Zolitschka, B., PASADO Science Team, 2011. The PASADO core processing strategy – a proposed new protocol for sediment treatment in multidisciplinary lake drilling projects. *Sedimentary Geology* 239, 104–115.
- Orsi, T.H., Edwards, C.M., Anderson, A.L., 1994. X-ray computed tomography: a nondestructive method for quantitative analysis of sediment cores. *Journal of Sedimentary Research A* 64, 690–693.
- Orsi, T.H., Anderson, A.L., 1999. Bulk density calibration for X-ray tomographic analyses of marine sediments. *Geo-Marine Letters* 19 (4), 270–274.
- Paillard, D., 1996. Macintosh Program performs time-series analysis. *Eos Transactions AGU* 77 (39), 379. <http://dx.doi.org/10.1029/96EO00259>.
- St-Onge, G., Long, B., 2009. CAT-scan analysis of sedimentary sequences: an ultrahigh-resolution paleoclimatic tool. *Engineering Geology* 103, 127–133.
- St-Onge, G., Mulder, T., Francus, P., Long, B., 2007. Continuous physical properties of cored marine sediments. In: Hillaire-Marcel, C., de Vernal, A. (Eds.), *Proxies in Late Cenozoic Paleoceanography*. Elsevier, pp. 63–98.
- Tamari, S., 2004. Optimum design of the constant-volume gas pycnometer for determining the volume of solid particles. *Measurement Science and Technology* 15, 549–558.
- Tanaka, A., Nakano, T., Ikehara, K., 2011. X-ray computerized tomography analysis and density estimation using a sediment core from the challenger mound area in the porcupine seabight, off western Ireland. *Earth, Planets and Space* 63 (2), 103–110.
- Thompson, J., Croudace, I.W., Rothwell, R.G., 2006. A Geochemical Application of the ITRAX Scanner to a Sediment Core Containing Eastern Mediterranean Sapropel Units, *New Ways of Looking at Sediment Cores and Core Data*, pp. 65–77.
- Zolitschka, B., Anselmetti, F., Ariztegui, D., Corbella, H., Francus, P., Ohlendorf, C., Schäbitz, F., Team, T.P.S.D., 2009. The Laguna Potrok Aike Scientific Drilling Project PASADO (ICDP Expedition 5022). *Scientific Drilling* 8.